Digital signal propagation in dispersive media

P. M. Jordan and Ashok Puri[a)]
Department of Physics, University of New Orleans, New Orleans, Louisiana 70148

(Received 13 August 1998; accepted for publication 23 October 1998)

In this article, the propagation of digital and analog signals through media which, in general, are both dissipative and dispersive is modeled using the one-dimensional telegraph equation. Input signals are represented using impulsive, Heaviside unit step, Gaussian, rectangular pulse, and both unmodulated and modulated sinusoidal pulse type boundary data. Applications to coaxial transmission lines and freshwater signal propagation, for both digital and analog signals, are included. The analysis presented here supports the finding that digital transmission in dispersive media is generally superior to that of analog. The boundary data (input signals) give rise to solutions of the telegraph equation which contain propagating discontinuities. It is shown that the magnitudes of these discontinuities, as a function of distance, can be found without the need of solving the governing equation. Thus, for digital signals in particular, signal strength at a given distance from the input source can be easily determined. Furthermore, the magnitudes of these discontinuities are found to be independent of both the dispersion coefficient k and the elastic coefficient b. In addition, it is shown that, depending on the algebraic sign of k, one of two distinct forms of dispersion is possible and that for small-time intervals, solutions are approximately independent of k. © *1999 American Institute of Physics.* [S0021-8979(99)03803-7]

I. INTRODUCTION

In 1876, the telegraph equation,

$$\frac{\partial^2 u}{\partial x^2}-\frac{1}{c^2}\frac{\partial^2 u}{\partial t^2}-\gamma\frac{\partial u}{\partial t}-b^2u=0, \tag{1.1}$$

where c is a positive constant and γ and b are nonnegative constants, was investigated by Heaviside in his research on coaxial marine telegraph cables[1] (see also Doetsch[2] and Bland[3]). This equation describes phenomena in a vast array of fields. For example, it appears in the theory of superconducting electrodynamics where it describes the propagation of electromagnetic waves in superconducting media.[4] The telegraph equation also has a central role in the study of excitons.[5] The telegraph equation has applications in the biological sciences as well. In cases where linearization of the leakage conductance is justified, the telegraph equation is the governing equation for the transmission of electrical impulses in the axons of nerve and muscle cells.[1] It governs the propagation of pressure waves which occur in pulsatile blood flow in arteries.[6] The telegraph equation also describes the random, one-dimensional motion of insects along a hedge[6] (a generalization of the random walk problem[7]). Special cases of it arise in almost all branches of physics. Taking $\gamma=b=0$ gives the classical wave equation with phase velocity c. Taking $b=0$ gives the damped wave equation. This equation describes the propagation of thermal waves, at finite speeds, in a thermally conducting medium (by the Maxwell–Cattaneo theory[8–10]), the propagation of electromagnetic waves in an electrically conducting (hence absorbing) medium,[11] and the classic form of the random walk problem.[7] Finally, taking $\gamma=0$, $b^2=m_0^2c_0^2/\hbar^2$ and $c=c_0$, where c_0 is the speed of light in free space, m_0 is the particle's rest mass, and $\hbar$ is Planck's constant divided by 2π, the telegraph equation becomes the one-dimensional Klein–Gordon or relativistic wave equation.[12,13] It is the correct wave equation for a spinless relativistic particle and is therefore regarded as the governing equation for the scalar meson field.[12]

In this work, we examine the propagation of electromagnetic waves in media which, in general, are both conducting and dispersive. In particular, we are interested in developing a deeper understanding of digital transmission in such media. Understanding of how digital signals evolve over time in dispersive/conducting media is of much interest because of the many diverse applications, e.g., in the fields of medicine, electromagnetic wave propagation, and communications. In Sec. II, we present a model system and solve Eq. (1.1) for arbitrary input signals using the Laplace transformation method. Section III contains numerical results for the following input signals and various values of the time and solution parameters: the Heaviside unit step, Gaussian rectangular pulse, and unmodulated sinusoidal pulse. A comparison of analog to digital signal propagation through a semi-infinite coaxial transmission line, and an infinite conducting medium, is presented in Sec. IV. In Sec. V, we determine the magnitudes of the discontinuities using the method of Boley[14] and a connection is made to digital signal strength. This sheds new light on how to devise a transmission line based on digital signal strength at a given location. Finally, Sec. VI is devoted to a brief discussion and conclusions follow in Sec. VII.

II. MODEL SYSTEM

Consider an initially quiescent, homogeneous and isotropic, electrically conducting dispersive medium occupying the

a)Electronic mail: apuri@uno.edu

half-space $x>0$. At the $x=0$ boundary, a time-dependent input signal is applied. This system is modeled by the following initial-boundary value problem (IBVP) involving the telegraph equation:

$$u_{xx}-u_{\tau\tau}-ru_{\tau}-b^2u=0, \quad x,\tau>0, \tag{2.1}$$

$$u(\infty,\tau)=0, \quad u(0,\tau)=F(\tau), \quad \tau>0, \tag{2.2}$$

$$u(x,0)=u_{\tau}(x,0)=0, \quad x>0, \tag{2.3}$$

where $u=u(x,\tau)$ is any component of the electric field vector, $r=c\gamma$ is the damping coefficient, b is the elastic coefficient, $\tau=ct$ (giving a phase velocity of unity), and $F(\tau)$ is the input signal.

Applying the Laplace transformation with respect to τ to Eq. (2.1) and employing initial data, Eq. (2.3), we obtain

$$\frac{d^2\mathcal{L}(u)}{dx^2}-(s^2+rs+b^2)\mathcal{L}(u)=0, \tag{2.4}$$

where $\mathcal{L}(\cdot)$ is the Laplace transform operator and s is the transform parameter. Solving Eq. (2.4), we get the transform domain solution

$$\mathcal{L}(u)=f(s)\exp[-x\sqrt{(s+r/2)^2+k}], \tag{2.5}$$

where $k=b^2-r^2/4$ is known as the *dispersion coefficient* and

$$\mathcal{L}[u(0,\tau)]=\mathcal{L}[F(\tau)]\equiv f(s), \tag{2.6}$$

and where $f(s)$ exists. Thus using a table of inverse Laplace transforms[15] and the inverse Laplace transform convolution theorem,[15] we find that for all allowable $F(\tau)$, the τ-domain solution is

$$u(x,\tau)=\theta(\tau-x)\begin{cases} e^{-rx/2}F(\tau-x)-\displaystyle\int_x^{\tau}F(\tau-\eta)K_J(x,\eta,k)\,d\eta, & \text{if } k>0,\\ e^{-rx/2}F(\tau-x), & \text{if } k=0,\\ e^{-rx/2}F(\tau-x)+\displaystyle\int_x^{\tau}F(\tau-\eta)K_I(x,\eta,|k|)\,d\eta, & \text{if } k<0,\end{cases} \tag{2.7}$$

where $\theta(\cdot)$ is the Heaviside unit step function,

$$K_J(x,\eta,k)=x\sqrt{k}e^{-r\eta/2}\frac{J_1[\sqrt{k(\eta^2-x^2)}]}{\sqrt{\eta^2-x^2}}, \tag{2.8}$$

$$K_I(x,\eta,|k|)=x\sqrt{|k|}e^{-r\eta/2}\frac{I_1[\sqrt{|k|(\eta^2-x^2)}]}{\sqrt{\eta^2-x^2}}, \tag{2.9}$$

and where $J_1(\cdot)$ is Bessel's function of the first kind of order one and $I_1(\cdot)$ is the modified Bessel function of the first kind of order one. The solution $u(x,\tau)$ consists of two terms. The first shows that the boundary data are attenuated as they are propagated into the solution domain. The second term vanishes for $k=0$ and represents the effects of dispersion (i.e., the dependence of phase velocity on frequency). It may be thought of as a ''tail'' [3] following the first term. Observe that if $u(0,0)=F(0)\neq 0$ then the boundary data will be discontinuous. This is due to the fact that the initial conditions were taken as $u(x,0)=u_{\tau}(x,0)=0$. Since the telegraph equation is hyperbolic in nature, this discontinuity in boundary data is propagated into the solution domain. Hence $u(x,\tau)$ is also discontinuous. The graphs shown in Figs. 1(a) and 1(b) are those of K_J and K_I, respectively, for $\tau=2.00$. The broken vertical line at $x=2.0$ in each graph indicates where the discontinuity caused by the Heaviside function multiplying each of the kernels would occur; to the right of it ($x>\tau$) both plots would be zero. Physically, this shows that causality is satisfied. Why this is so mathematically can be seen by fixing $\tau>0$ at $\tau=\tau_0$ and letting x vary. The Heaviside function $\theta(\tau_0-x)$ must then be replaced by $\theta(x)-\theta(x-\tau_0)$. Finally, the presence of the Heaviside function also serves to suppress the unbounded growth exhibited by K_J as x becomes large.

III. NUMERICAL RESULTS

Here we give Mathematica[16] generated graphs of solution (2.7) for the following input signals $F(\tau)$:

(1) Heaviside unit step $F(\tau)=\theta(\tau)$,
(2) Gaussian $F(\tau)=\theta(\tau)e^{-m^2\tau^2}$,
(3) Rectangular pulse $F(\tau)=M[\theta(\tau)-\theta(\tau-p)]$,
(4) Unmodulated sinusoidal pulse $F(\tau)=[\theta(\tau)-\theta(\tau-p)]\sin(\pi\tau/p)$,

where the positive constants M, m, and p denote the pulse magnitude, the decay coefficient, and the pulse width, respectively. Note that, with the exception of Fig. 4, we have adopted the following convention here in Sec. III: a broken curve corresponds to the dispersion coefficient $k>0$, a bold curve to $k<0$, and a thin solid curve to $k=0$. Finally, Figs. 3 and 4 were plotted for $p=1.50$.

A. Small-time behavior

In Figs. 2(a)–2(c) are shown plots for Heaviside, Gaussian, and unmodulated sinusoidal pulse inputs for $\tau=0.50$ and all three cases of k. Note that in each plot, the curves for all three cases of k lie very close to each other. Furthermore, note that by inverting the large s expansions given in the Appendix, we can obtain small-τ expressions of Eq. (2.7) for the various $F(\tau)$. For example, the small-τ expressions corresponding to Figs. 2(a)–2(c) are

$$\text{(a)}\quad u(x,\tau)=e^{-rx/2}\theta(\tau-x)\left(1-\frac{kx}{2}(\tau-x)+\frac{k^2x^2}{16}(\tau-x)^2-\cdots\right), \tag{3.1}$$

$$\text{(b)}\quad u(x,\tau)=e^{-rx/2}\theta(\tau-x)\left(1-\frac{kx}{2}(\tau-x)-m^2(\tau-x)^2+\cdots\right), \tag{3.2}$$

$$\text{(c)}\quad u(x,\tau)=\frac{\pi}{p}e^{-rx/2}\theta(\tau-x)\left[(\tau-x)-\frac{kx}{4}(\tau-x)^2+\left(\frac{x^2k^2}{48}-\frac{\pi^2}{6p^2}\right)(\tau-x)^3+\cdots\right]$$
$$+\frac{\pi}{p}e^{-rx/2}\theta(\tau-x-p)\left[(\tau-x-p)-\frac{kx}{4}(\tau-x-p)^2+\left(\frac{x^2k^2}{48}-\frac{\pi^2}{6p^2}\right)(\tau-x-p)^3+\cdots\right]. \tag{3.3}$$

From Eqs. (3.1)–(3.3), one can clearly see that k does not appear in the first (dominant) term of any of any of these series. Hence, for small τ (time), we conclude that u is approximately independent of k.

B. Effects of dispersion on pulse-type inputs

In Figs. 3(a), and 3(b) with $\tau=2.00$ $M=1.00$, and $p=1.50$, we can clearly see the dispersive tail in the plots of both the rectangular pulse and the unmodulated sinusoidal pulse, respectively. Note that for $k<0$, the tail lies above the x axis while for $k>0$, it lies below (for $k=0$, the tail does not exist). In addition, we see that the $k=0$ curve lies above the $k>0$ curve and below the $k<0$ curve. Furthermore, while the rectangular pulse is clearly discontinuous, the unmodulated sinusoidal pulse is continuous everywhere. The development of the dispersive tail (for $k<0$) as a function of τ, for both rectangular and modulated sinusoidal pulse data, will be demonstrated in Sec. IV.

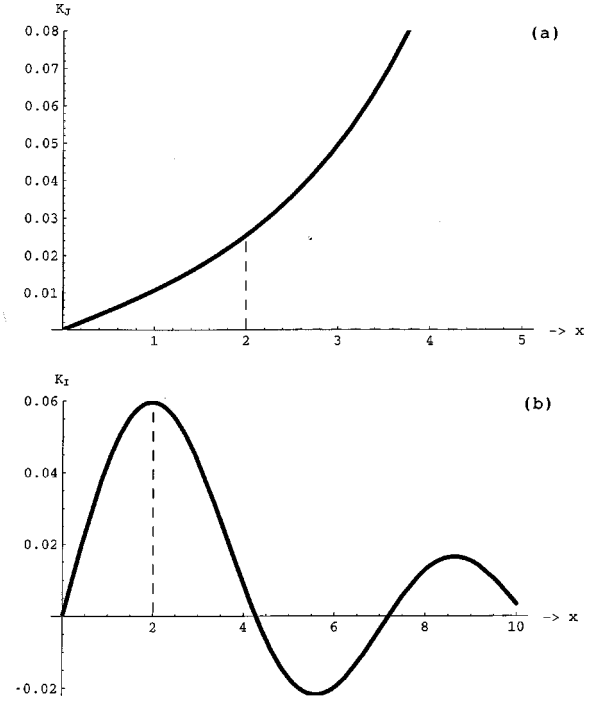

FIG. 1. For $\tau=2.0$ and $r=2.85$: (a) K_J vs x, $k=0.44$; (b) K_I vs x, $k=-1.03$.

C. Effects of elastic and damping coefficients

Figures 4(a) and 4(b) show, respectively, the effects of varying the elastic coefficient b and damping coefficient r, with $k=-1.03$ fixed, for a rectangular pulse. In Fig. 4(a) r is fixed at 2.85 and we use the following convention for the plotted curves: broken$\Rightarrow b=0.50$, bold$\Rightarrow b=1.00$, and solid$\Rightarrow b=1.25$. In Fig. 4(a) observe that increasing (de-

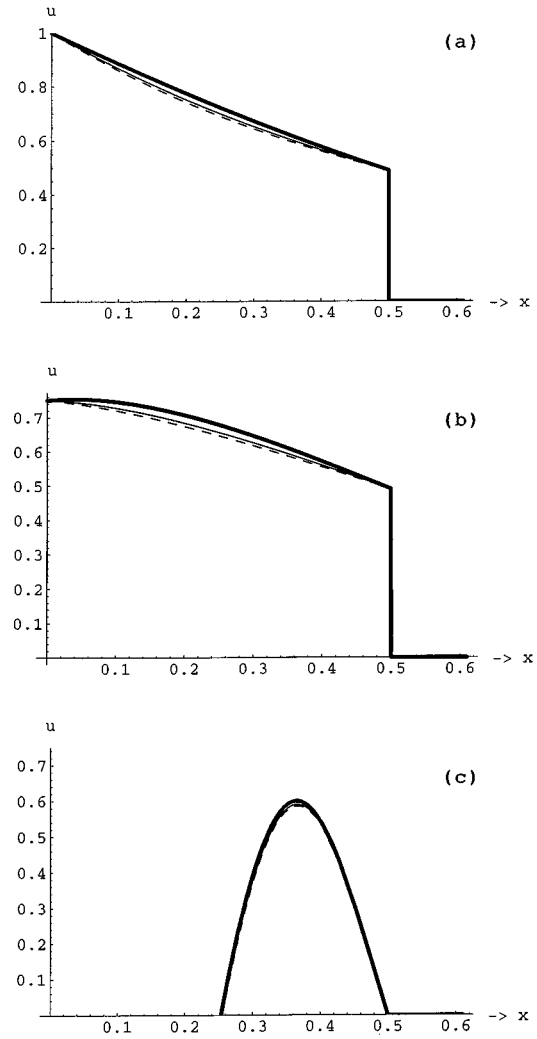

FIG. 2. u vs x for $\tau=0.50$ and $r=2.85$. Bold line: $k=-1.03$; solid line: $k=0$; broken line: $k=0.44$. (a) Heaviside; (b) Gaussian with $m=1.00$; (c) unmodulated sinusoidal pulse with $p=1.50$.

creasing) b decreases (increases) the area under the dispersive tail, the area under the pulse, and the magnitude of the trailing edge of the pulse. Note, however, that varying the elastic coefficient has little or no effect on the leading edge. For Fig. 4(b), b is fixed at 1.00 and the convention for the plotted curves is as follows: broken$\Rightarrow r=2.25$, bold$\Rightarrow r=2.85$, and solid$\Rightarrow r=3.35$. As would be expected, increasing (decreasing) r decreases (increases) pulse magnitude, at both trailing and leading edges, and the area under the pulse while increasing (decreasing) the area bounded by the dispersive tail.

IV. PHYSICAL APPLICATIONS

We now consider two physical applications. In both of these examples we will focus on the case of $k<0$. The case of $k<0$ is of much interest as it occurs in transmission line applications and has the potential for the greatest impact on digital transmission in dispersive media.

A. Coaxial transmission line

Consider a simplified model of a coaxial transmission line. Equation (1.1) is the governing equation for both current and voltage in such a line with no external driving.[1–3] Expressing the constants c, γ, and b in Eq. (1.1) in terms of the electrical parameters L, R, C, and G we find

$$c=(LC)^{-1/2}, \quad \gamma=LG+RC, \quad b^2=RG, \tag{4.1}$$

where, per unit length, we have inductance $L>0$, resistance $R\geqslant 0$, capacitance $C>0$, and $G\geqslant 0$ is the leakage conductance between the two wires. Thus, Eq. (1.1) becomes

$$\frac{\partial^2 u}{\partial x^2}-LC\,\frac{\partial^2 u}{\partial t^2}-(LG+RC)\,\frac{\partial u}{\partial t}-RGu=0. \tag{4.2}$$

In terms of the electrical parameters, the dispersion coefficient k is given by

$$k=-\frac{(RC-LG)^2}{4LC}. \tag{4.3}$$

Hence for a coaxial transmission line, we have $k\leqslant 0$ always. This was also shown by Doetsch[2] and by Bland.[3] Thus Eq. (4.2) admits, at most, only one form of dispersion. In his research, Heaviside found that by designing a marine cable such that $RC=LG$, he could produce a ''distortionless'' marine transmission line. Over the years, such lines came to be known as Heavified lines.[1] Thus $k=0$ corresponds to a Heavified transmission line. As can be seen from solution (2.7), an input signal propagating down such a line is attenuated, but experiences no dispersive effects (i.e., it is reduced in magnitude but maintains its form). In contrast, for $k<0$ an input signal is not only attenuated, but also suffers from dispersion. This dispersive effect is represented by the corresponding integral term given in solution (2.7).

Figures 5 and 6 illustrate, respectively, the τ evolution of solution (2.7) for the rectangular and modulated sinusoidal pulses,

$$F(\tau,p)=M[\theta(\tau)-\theta(\tau-p)],$$

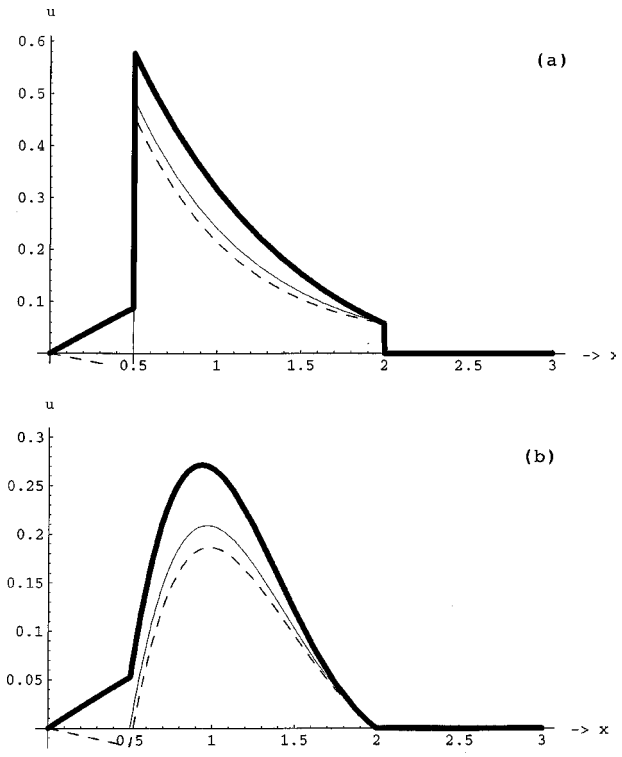

FIG. 3. u vs x for $\tau=2.00$, $r=2.85$, and $p=1.50$. Bold: $k=-1.03$; solid: $k=0$; broken: $k=0.44$. (a) Rectangular pulse with $M=1.00$; (b) unmodulated sinusoidal pulse.

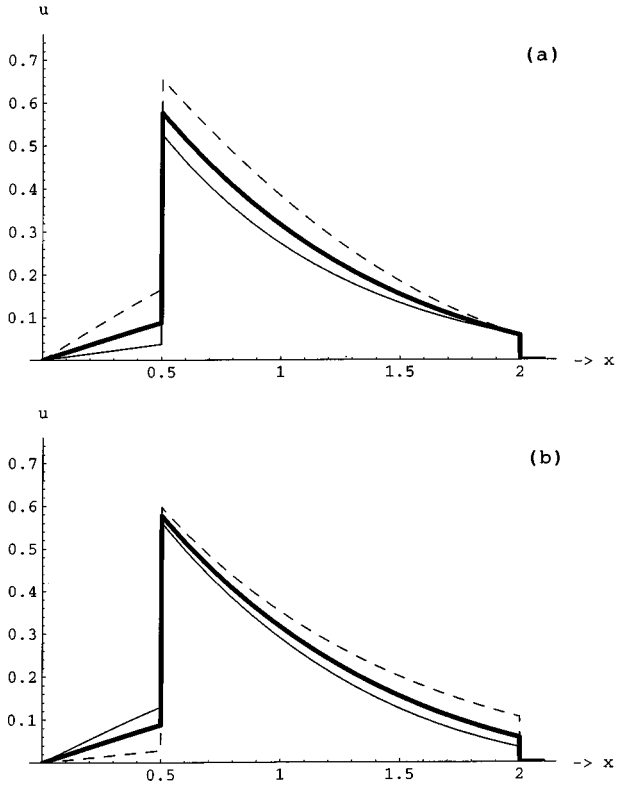

FIG. 4. u vs x for a rectangular pulse with $\tau=2.00$, $M=1.00$, and $p=1.50$. (a) $r=2.85$ (fixed). Broken: $b=0.50$; bold: $b=1.00$; solid: $b=1.25$. (b) $b=1.00$ (fixed). Broken: $r=2.25$; bold: $r=2.85$; solid: $r=3.35$.

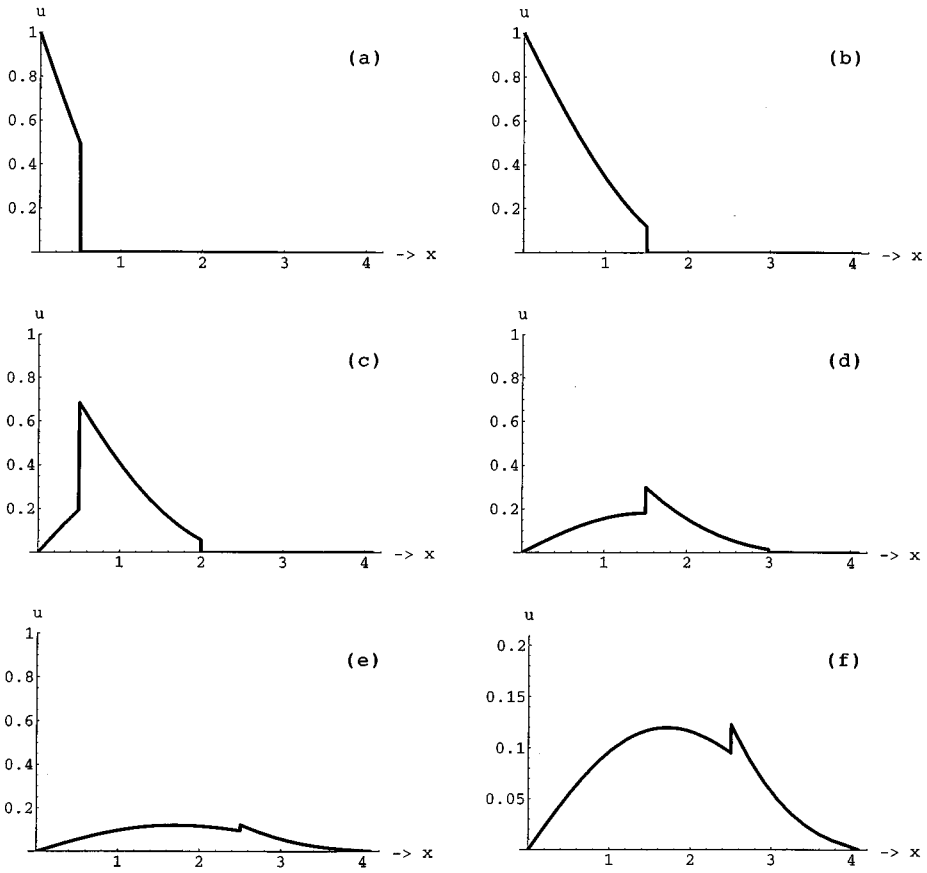

FIG. 5. u vs x for a rectangular pulse with $k=-2.02$, $r=2.85$, $b=0.1$, $M=1.00$, and $p=1.50$. (a) $\tau=0.50$; (b) $\tau=1.50$; (c) $\tau=2.00$; (d) $\tau=3.00$; (e),(f) $\tau=4.00$.

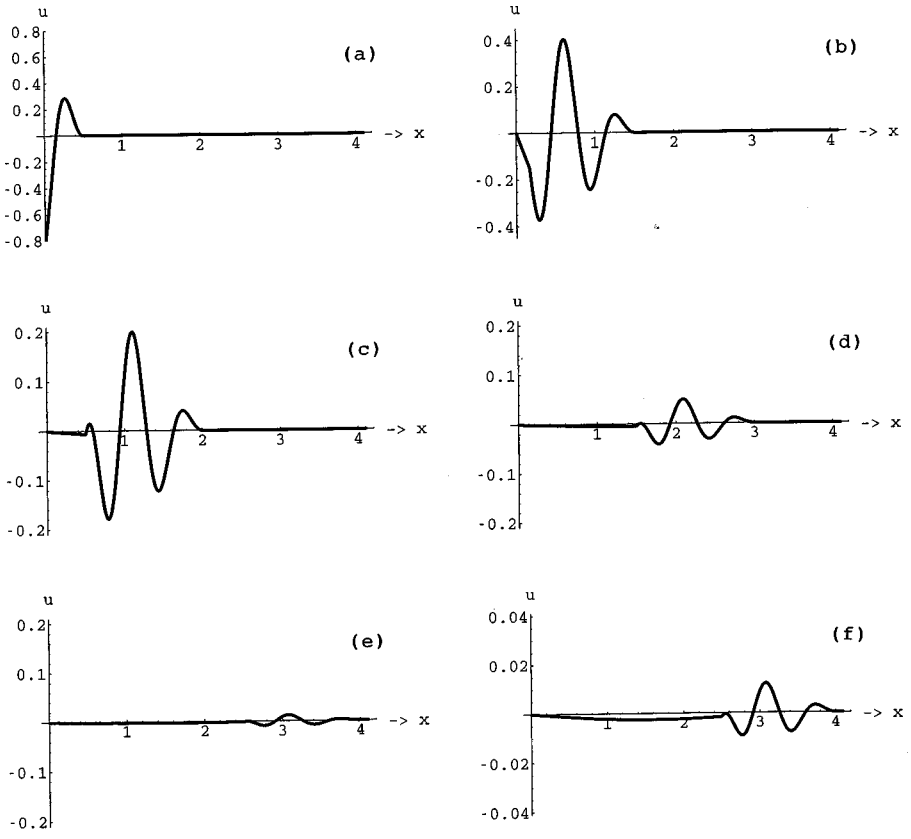

FIG. 6. u vs x for a modulated sinusoidal pulse with $k=-2.02$, $r=2.85$, $b=0.1$, $\omega=9.00$, $q=2\pi/3$, and $p=1.50$. (a) $\tau=0.50$; (b) $\tau=1.50$; (c) $\tau=2.00$; (d) $\tau=3.00$; (e),(f) $\tau=4.00$.

and

$$F(\tau,p)=[\theta(\tau)-\theta(\tau-p)]\sin(\omega\tau)\sin(q\tau), \tag{4.4}$$

where $\omega>q$ are positive constants. Figures 5(a)–5(e) and 6(a)–6(e) correspond to $\tau=0.50$, 1.50, 2.00, 3.00, and 4.00 while Figs. 5(f) and 6(f) are magnified views of Figs. 5(e) and 6(e), respectively. Clearly Figs. 5 and 6 could, respectively, represent a digital pulse and a short modulated analog signal, with carrier frequency ω and modulation frequency q, propagating down a semi-infinite coaxial transmission line with electrical parameters L, R, C, and G chosen in such a way that Eq. (4.3) yields $k=-2.02$. In Figs. 5 and 6, we see that upon entering the medium both inputs suffer heavy attenuation. By $\tau=2.00$, a tail has developed on each signal. Observe in Fig. 5(e) how a discernible digital signal is still present at $\tau=4.00$, whereas at $\tau=4.00$ the analog signal is almost imbedded in the noise of its dispersive tail [Fig. 6(e)].

B. Infinite conducting medium

Consider a conducting medium of infinite extent which is both homogeneous and isotropic, for example, a large deep freshwater lake. Somewhere in this medium is a spherical cavity of radius a. Starting at time $t=0$ and ending at $t=\not{\tau}$ an electromagnetic pulse $F(t,\not{\tau})$ is transmitted from the surface of the cavity ($\rho=a$), into the medium (e.g., from a deeply submerged radio transmitter). We wish to describe the pulse at any later time. Let us place the origin of a spherical coordinate system at the center of this cavity. The IBVP we must solve is

$$\frac{1}{\rho^2}\frac{\partial}{\partial\rho}\left(\rho^2\frac{\partial u}{\partial\rho}\right)-\frac{n^2}{c_0^2}\frac{\partial^2 u}{\partial t^2}-\mu\sigma\frac{\partial u}{\partial t}=0,\quad \rho>a,\quad t>0, \tag{4.5}$$

$$u(a,t)=F(t,\not{\tau}),\quad u(\infty,t)=0,\quad t>0, \tag{4.6}$$

$$u(\rho,0)=u_t(\rho,0)=0,\quad \rho>a, \tag{4.7}$$

where n, μ, and σ are the refractive index, permeability, and conductivity, respectively, of the medium, and $\not{\tau}$ is the pulse width of the input signal. Equation (4.5) is known as the spherically symmetric damped wave equation. A derivation of the general case of Eq. (4.5) is given by Born and Wolf.[11] Let us solve IBVP Eqs. (4.5)–(4.7) for both digital and analog signal inputs F. Substituting $u=U/\rho$, $\tau=vt$, where $v=c_0/n$, and $r=\sigma\mu v$ IBVP Eqs. (4.5)–(4.7) become

$$U_{\rho\rho}-U_{\tau\tau}-rU_\tau=0,\quad \rho>a,\quad \tau>0, \tag{4.8}$$

$$U(a,\tau)=aF(\tau,p),\quad U(\infty,\tau)=0,\quad \tau>0, \tag{4.9}$$

$$U(\rho,0)=U_\tau(\rho,0)=0,\quad \rho>a, \tag{4.10}$$

where $p=v\not{\tau}$. Clearly Eq. (4.8) corresponds to Eq. (2.1) with $b=0$. Hence $k=-r^2/4$ and the solution follows using the $k<0$ case of Eq. (2.7).

(i) Rectangular (digital) pulse propagation. For $F(\tau,p)=[\theta(\tau)-\theta(\tau-p)]$, we have

$$\begin{aligned}u(\rho,\tau)=\frac{a}{\rho}e^{-r(\rho-a)/2}&[\theta(\tau-\rho+a)-\theta(\tau-p-\rho+a)]\\&+\frac{ar(\rho-a)}{2\rho}\Bigg[\theta(\tau-\rho+a)\\&\times\int_{\rho-a}^{\tau}K(\rho-a,\eta,r)\,d\eta-\theta(\tau-\rho+a-p)\\&\times\int_{\rho-a}^{\tau-p}K(\rho-a,\eta,r)\,d\eta\Bigg],\end{aligned} \tag{4.11}$$

where $K(\rho-a,\eta,r)$, the kernel of the Laplace transform convolution integral, is given by

$$K(\rho-a,\eta,r)=e^{-r\eta/2}\frac{I_1[(r/2)\sqrt{\eta^2-(\rho-a)^2}]}{\sqrt{\eta^2-(\rho-a)^2}}. \tag{4.12}$$

(ii) Analog pulse propagation. Taking $F(\tau,p)=[\theta(\tau)-\theta(\tau-p)]\sin(\omega\tau)\sin(\omega\tau)$ we obtain

$$\begin{aligned}u(\rho,\tau)=\frac{a}{\rho}e^{-r(\rho-a)/2}&[\theta(\tau-\rho+a)\sin[w(\tau-\rho+a)]\sin[q(\tau-\rho+a)]-\theta(\tau-p-\rho+a)\sin[w(\tau-\rho+a)]\sin[q(\tau-\rho+a)]]\\&+\frac{ar(\rho-a)}{2\rho}\Bigg[\theta(\tau-\rho+a)\int_{\rho-a}^{\tau}\sin[w(\tau-\eta)]\sin[q(\tau-\eta)]K(\rho-a,\eta,r)\,d\eta-\theta(\tau-\rho+a-p)\\&\times\int_{\rho-a}^{\tau-p}\sin[w(\tau-\eta)]\sin[q(\tau-\eta)]K(\rho-a,\eta,r)\,d\eta\Bigg].\end{aligned} \tag{4.13}$$

We note that Eq. (4.13) is valid for all $\omega,q>0$. The plots in Figs. 7 and 8 show u vs $\rho-a$. They illustrate the τ evolution of Eqs. (4.11) and (4.13), respectively, for $r=0.84$, $a=0.50$, $p=1.50$, $q=2\pi/3$, and $\omega=5q$. The corresponding medium parameters used are for freshwater are $n=9.00$ [$\Rightarrow v=(1/3)\times10^8$ m/s], and $\sigma=0.02$ mho/m. Furthermore we have ω corresponding to a carrier frequency of 55.50 MHz, q corresponding to a modulation frequency of 11.10 MHz, and we have taken a pulse width of $\not{\tau}=4.50\times10^{-8}$ s. Again we see attenuation quickly reduces the magnitude of both the digital and analog inputs. In addition we note that while the digital pulse develops a tail (Fig. 7), it is apparent from Fig. 8 that the tail associated with the analog pulse is not noticeable. Initially, this seems to be due to the fact that ω is an odd-integer multiple of q. However, numerical work carried out but not presented here suggests that this is also true when ω is an even-integer multiple of q. Hence, it appears that when ω is an integer multiple of q, the

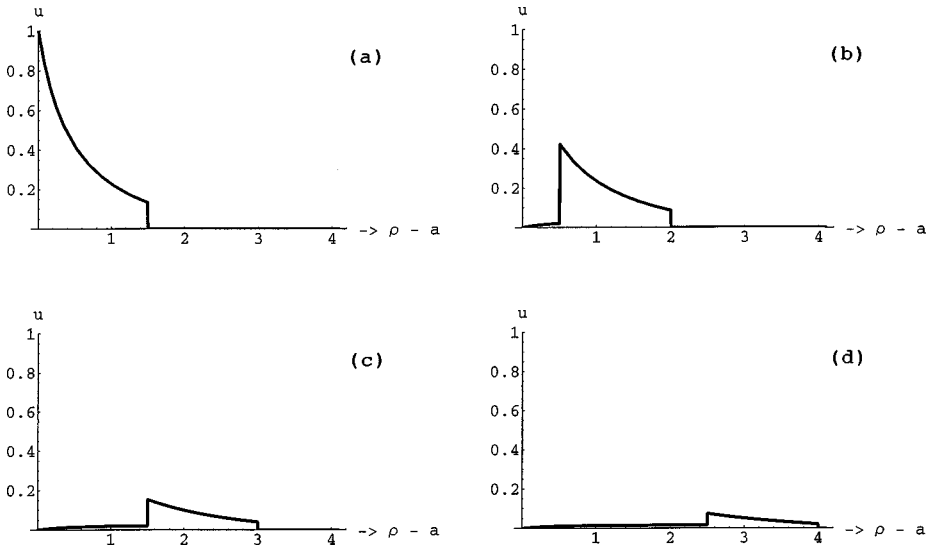

FIG. 7. u vs $\rho-a$ for a rectangular pulse with $a=0.50$, $r=0.84$, $M=1.00$, and $p=1.50$. (a) $\tau=1.50$; (b) $\tau=2.00$; (c) $\tau=3.00$; (d) $\tau=4.00$.

two integrals appearing in Eq. (4.13) are nearly equal, resulting in a near cancellation of the dispersive part of the solution for $\tau>(\rho-a)+p$. Last, it is clear that for both digital and analog inputs there exist critical distances past which both become lost in the background noise and tail.

Figures 5 and 6 support the notion that digital transmission is generally preferred over analog in dispersive media. Whereas a digital detector will sense only a high low signal input, and will therefore ''miss'' the dispersive tail, an analog detector, by its very nature, will sense both the intended wave form and its dispersive tail which, inevitably, will appear as degraded output. However, Fig. 8 indicates that for the example considered here dispersive effects on an analog signal can be reduced by picking the carrier frequency to be an integer multiple of the modulation frequency.

V. DISCONTINUITIES

Knowledge of discontinuities is extremely important to researchers in many areas of physics. For example, in digital systems we often encounter signals composed of a series of rectangular pulses. Clearly such signals can be regarded as discontinuous wave forms. As already noted, a rectangular digital input pulse of magnitude M and width p can be represented mathematically by

$$F(\tau)=M[\theta(\tau)-\theta(\tau-p)]. \tag{5.1}$$

Obviously Eq. (5.1) is a function with a jump discontinuity. Physically, the magnitude of the discontinuity (or saltus), which in this case is a constant M, indicates the signal strength of the pulse. However, as a digital pulse propagates in a absorbing/dispersive medium the signal strength of the pulse is reduced over distance.

Here in Sec. V, the method of Boley[14] (see also Puri and Kythe[10]) is used to determine the magnitudes of the propagating discontinuities present in u. The power of this approach is that the magnitude of a discontinuity present in a solution can be found without having to perform the often difficult tasks of first obtaining the time-domain solution u, and then taking the appropriate limits. Let us now give the precise statement of Boley's[14] criterion. Denote by $\mathcal{S}[g(x_0)]$ the saltus of a function $g(x)$ at a point x_0, i.e.,

$$\mathcal{S}[g(x_0)]=g(x_0+0)-g(x_0-0). \tag{5.2}$$

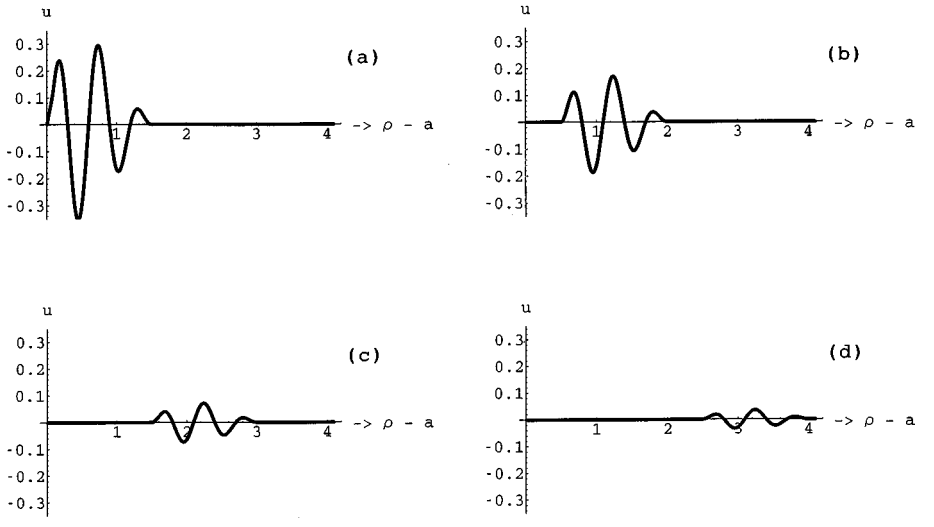

FIG. 8. u vs $\rho-a$ for a modulated sinusoidal pulse with $a=0.50$, $r=0.84$, $p=1.50$, $q=2\pi/3$, and $\omega=10\pi/3$. (a) $\tau=1.50$; (b) $\tau=2.00$; (c) $\tau=3.00$; (d) $\tau=4.00$.

TABLE I. Discontinuities in u: Impulsive, Heaviside, and Gaussian inputs.

$F(\tau)$	$\delta(\tau)$	$\theta(\tau)$	$\theta(\tau)e^{-m^2\tau^2}$
Wave front	$x=\tau$	$x=\tau$	$x=\tau$
$\mathcal{S}[u]$	∞	$e^{-rx/2}$	$e^{-rx/2}$
$\mathcal{S}[u_\tau]$	∞	∞	∞
$\mathcal{S}[u_x]$	∞	∞	∞

Suppose that

$$Q(x,\tau)=\frac{1}{2\pi i}\int_{\alpha-i\infty}^{\alpha+i\infty}[\Omega(x,s)h(x)e^{-s\kappa x}]e^{s\tau}ds, \qquad (5.3)$$

where $\Omega(x,s)$ is an infinite series in powers of $1/s$, the function $h(x)\neq 0$ is real valued and bounded for $x\geqslant 0$, κ is a positive constant, and α is a constant chosen in the standard manner of the inverse Laplace transform.[15] Then the saltus of the function Q is given by the following criterion:
If

$$\lim_{s\to\infty} s^N\left[\Omega(x,s)-\frac{1}{s^n}\right]=0, \quad n\geqslant 0, \quad N\geqslant 1, \qquad (5.4)$$

then

$$\mathcal{S}[Q(x,\tau)]=\begin{cases} 0 & \text{for } \kappa x-\tau\neq 0, \\ \begin{cases} 0 & \text{if } n>1, \\ h(x) & \text{if } n=1, \\ \infty & \text{if } n<1, \end{cases} & \text{for } \kappa x-\tau=0. \end{cases} \qquad (5.5)$$

We illustrate the use of Boley's method by applying it to the large s expansions given in the Appendix [Eqs. (A1)–(A6)]; we can determine the propagating discontinuities occurring in u and its derivatives for the various $F(\tau)$ considered. We give these results, up to first derivatives, in Tables I and II. Table I contains the following input signals (boundary data): impulsive, Heaviside unit step, and Gaussian, respectively. In Table II we have rectangular and unmodulated sinusoidal pulse input signals. Here $\delta(\cdot)$ is the Dirac delta (impulse) function and the quantity $\mathcal{S}[u_x]$ corresponding to the sinusoidal pulse input was determined using Hadamard's lemma[3]

$$\frac{D}{D\tau}(\mathcal{S}[u])=\mathcal{S}[u_x]+\mathcal{S}[u_\tau], \qquad (5.6)$$

where the operator $D/D\tau$ denotes differentiation with respect to τ following the wave front, and the continuity of u (i.e., $\mathcal{S}[u]=0$). Observe from Tables I and II that in every case the magnitude of the discontinuity is independent of k. Furthermore, in the case of rectangular pulse signal, we see that $\mathcal{S}[u]$ at τ and $\tau-p$ gives the signal strength of the pulse at the leading and trailing edges, respectively, without having to solve for the time-domain solution of the problem. Finally note that, with the exception of $F(\tau)=\delta(\tau)$, all the boundary data considered resulted in strong discontinuities[3] in u. For the telegraph equation, which is of second order, strong discontinuities are jump discontinuities which occur in u, or u_x and u_τ.

TABLE II. Discontinuities in u: Rectangular and sinusoidal pulse inputs.

$F(\tau)$	$M[\theta(\tau)-\theta(\tau-p)]$		$[\theta(\tau)-\theta(\tau-p)]\sin(\pi\tau/p)$	
Wave front	$x=\tau$	$x=\tau-p$	$x=\tau$	$x=\tau-p$
$\mathcal{S}[u]$	$Me^{-rx/2}$	$Me^{-rx/2}$	0	0
$\mathcal{S}[u_\tau]$	∞	∞	$\frac{\pi}{p}e^{-rx/2}$	$\frac{\pi}{p}e^{-rx/2}$
$\mathcal{S}[u_x]$	∞	∞	$\frac{-\pi}{p}e^{-rx/2}$	$\frac{-\pi}{p}e^{-rx/2}$

VI. DISCUSSION

(1) If dispersion is present in any solution of the telegraph equation, it can occur in only one of the two possible forms corresponding to $k\neq 0$. Furthermore, for small τ (time), the solution $u(x,\tau)$ is approximately independent of k (Fig. 2).

(2) In every case of boundary data considered, the $k=0$ curve was found to lie above the $k>0$ curve and below the $k<0$ curve, with the $k<0$ curve having the greatest deviation from the nondispersive ($k=0$) curve (Fig. 3). Thus it is clear that the presence of dispersion influences the magnitude of $u(x,\tau)$ and that these influences are opposite and unequal for the two forms of dispersion.

(3) For pulse-type boundary data dispersion causes a tail, extending from $x=0$ to the trailing edge of the pulse, to form (see Figs. 3–8). Thus, dispersion causes overall pulse width to increase with propagation distance.

(4) Decreasing (increasing) the elastic coefficient b increases (decreases) the area under the dispersive tail and the area under the pulse. In contrast, decreasing (increasing) the damping coefficient r decreases (increases) the area under the tail and increases (decreases) the area under the pulse (see Fig. 4).

(5) For rectangular pulse data, the leading edge of the pulse suffers greater attenuation than the trailing edge (Fig. 5). Hence depending on the detector, the initial pulse magnitude, and the propagation distance involved, a rectangular pulse could appear to arrive later than it would if dispersive effects were not present and the *detected* pulse width may appear less than the initial (input) pulse width.

(6) Figures 5–8 show that, for $k<0$, there is no significant qualitative difference between transmission line propagation of analog and digital pulses and the propagation of theses pulses in an infinite, homogeneous and isotropic conducting medium.

(7) Due to the formation of the dispersive tail and the different detection methods used in digital and analog systems, the analysis presented here generally supports the notion that digital transmission techniques are preferred over those of analog in a dispersive media. However, our analysis suggests that the dispersive tail can reduced if the carrier frequency is an integer multiple of the modulation frequency (Fig. 8).

(8) With the exception of $F(\tau)=\delta(\tau)$, all the boundary data considered produced strong discontinuities in u, i.e., jump discontinuities in u, or in u_x and u_τ as given in Tables I and II. These discontinuities propagate at the phase velocity

and decay exponentially over x with attenuation coefficient $r/2$.

(9) The magnitude of the discontinuity occurring in the solution (or its derivatives) of the telegraph equation is independent of both the dispersion coefficient k and elastic coefficient b; the discontinuity for both cases of $k \neq 0$ occurs only in the first (nonintegral) part of the solution.

VII. CONCLUSIONS

Our analysis demonstrates that the tail produced by the dispersive part of the solution is a major reason why digital transmission is generally preferred over conventional analog transmission. Digital detectors employ a threshold value to determine high and low signal strength (voltage). Thus, assuming the setting of the digital detector's threshold value allows for attenuation of the leading edge of the pulse and the presence of the dispersive tail, they are far less susceptible to the effects of dispersion. Analog detectors, however, sense an arriving wave form in a continuous manner; dispersive effects are incorporated with the input wave form in producing the output. The result, of course, is degradation of the reproduced signal (i.e., degraded output). However, our work suggests that for special values of the carrier and modulation frequencies the tail associated with an analog signal can be reduced. Furthermore, when small-time intervals are considered, our findings show that dispersion has little influence on the propagating signal.

We have shown (see Tables I and II) that the criterion of Boley[14] permits the determination of the propagating jumps, at a given location, without having to obtain the time-domain solution of the governing equation. This could prove useful to designers of digital systems which operate in dispersive media. The signal strength at both the leading and trailing edges of rectangular pulse data and *received* pulse width can be determined easily using Boley's method, and without any knowledge of the time-domain solution.

Although electrical signal propagation down copper transmission cables may, due to the advent of optical fibers, soon become a thing of the past, there is still a great deal to be learned in the area of bioelectromagnetic theory. The axons or long tendril portions of nerve and muscle cells behave much like marine cables.[1] An important difference, however, is that the leakage conductance in nerve axons is nonlinear.[1] Nevertheless, in cases where the leakage conductance can be linearized, an analysis similar to the one presented here could provide much insight into the workings of such biological ''transmission lines.''

ACKNOWLEDGMENTS

P.M.J. was funded by the Graduate Student Researchers Program of the National Aeronautics and Space Administration through the John C. Stennis Space Center, Training Grant No. NGT-13-52706. The authors would like to thank Professor Pratap Puri for his kind assistance and helpful comments.

APPENDIX: Large s expansions of transform domain solutions

For impulsive data:

$$\mathcal{L}(u) = \exp[-sx - rx/2]\left[1 - \frac{kx}{2s} + \frac{k^2x^2}{8s^2} - \cdots\right]. \tag{A1}$$

For Heaviside unit step data:

$$\mathcal{L}(u) = \exp[-sx - rx/2]\left[\frac{1}{s} - \frac{kx}{2s^2} + \frac{k^2x^2}{8s^3} - \cdots\right]. \tag{A2}$$

For Gaussian data:

$$\mathcal{L}(u) = \exp[-sx - rx/2]\left[\frac{1}{s} - \frac{kx}{2s^2} - \frac{2m^2}{8s^3} + \cdots\right]. \tag{A3}$$

For rectangular pulse data:

$$\begin{aligned}\mathcal{L}(u) = {} & M\ \exp[-sx - rx/2]\left[\frac{1}{2} - \frac{kx}{2s^2} + \frac{k^2x^2}{8s^3} - \cdots\right] \\ & - M\ \exp[-s(x+p) - rx/2] \\ & \times\left[\frac{1}{2} - \frac{kx}{2s^2} + \frac{k^2x^2}{8s^3} - \cdots\right].\end{aligned} \tag{A4}$$

For sinusoidal pulse data:

$$\begin{aligned}\mathcal{L}(u) = {} & \frac{\pi}{p}\exp[-sx - rx/2]\left[\frac{1}{s^2} - \frac{kx}{2s^3} + \left(\frac{x^2k^2}{8} - \frac{\pi^2}{p^2}\right)\frac{1}{s^4}\right. \\ & \left. + \cdots\right] + \frac{\pi}{p}\exp[-s(x+p) - rx/2] \\ & \times\left[\frac{1}{s^2} - \frac{kx}{2s^3} + \left(\frac{x^2k^2}{8} - \frac{\pi^2}{p^2}\right)\frac{1}{s^4} + \cdots\right],\end{aligned} \tag{A5}$$

and

$$\begin{aligned}\mathcal{L}(u_\tau) = {} & \frac{\pi}{p}\exp[-sx - rx/2]\left[\frac{1}{s} - \frac{kx}{2s^2} + \left(\frac{x^2k^2}{8} - \frac{\pi^2}{p^2}\right)\frac{1}{s^3}\right. \\ & \left. + \cdots\right] + \frac{\pi}{p}\exp[-s(x+p) - rx/2] \\ & \times\left[\frac{1}{s} - \frac{kx}{2s^2} + \left(\frac{x^2k^2}{8} - \frac{\pi^2}{p^2}\right)\frac{1}{s^3} + \cdots\right],\end{aligned} \tag{A6}$$

where Eq. (A6) was determined from Eq. (A5) using the relation

$$\mathcal{L}(u_\tau) = s\mathcal{L}(u). \tag{A7}$$

[1] H. M. Lieberstein, *Theory of Partial Differential Equations* (Academic, New York, 1972).
[2] G. Doetsch, *Introduction to the Theory and Application of the Laplace Transformation* (Springer, Berlin, 1974).
[3] D. R. Bland, *Wave Theory and Applications* (Oxford, London, 1988).
[4] P. R. Wallace, *Mathematical Analysis of Physical Problems* (Dover, New York, 1984).
[5] J. L. Birman, in *Excitons*, edited by E. I. Rashba and M. D. Sturge (North-Holland, Amsterdam, 1982).
[6] L. Debnath and P. Mikusiński, *Introduction to Hilbert Spaces with Applications* (Academic, San Diego, 1990).
[7] S. Goldstein, Q. J. Mech. Appl. Math. **4**, 129 (1951).
[8] D. S. Chandrasekharaiah, Appl. Mech. Rev. **39**, 355 (1986).

[9] D. D. Joseph and L. Preziosi, Rev. Mod. Phys. **61**, 41 (1989); **62**, 375 (1990).
[10] P. Puri and P. K. Kythe, Q. Appl. Math. **55**, 167 (1997).
[11] M. Born and E. Wolf, *Principles of Optics*, 3rd ed. (Pergamon, London, 1965).
[12] H. A. Enge, *Introduction to Nuclear Physics* (Addison–Wesley, Reading, MA, 1966).
[13] F. W. Byron and R. W. Fuller, *Mathematics of Classical and Quantum Physics* (Dover, New York, 1992), Vols. I and II.
[14] B. A. Boley, Q. Appl. Math. **19**, 273 (1962).
[15] R. V. Churchill, *Operational Mathematics*, 3rd ed. (McGraw–Hill, New York, 1972).
[16] S. Wolfram, *The Mathematica Book*, 3rd ed. (Wolfram Media/Cambridge University Press, New York, 1996).